PCCP

PAPER

View Article Online
View Journal | View Issue

Cite this: *Phys. Chem. Chem. Phys.*, 2016, **18**, 3124

Reducing the $V_2O_3(0001)$ surface through electron bombardment – a quantitative structure determination with *I*/*V*-LEED†

Felix E. Feiten, Helmut Kuhlenbeck* and Hans-Joachim Freund

Received 30th November 2015,
Accepted 22nd December 2015

DOI: 10.1039/c5cp07390a

www.rsc.org/pccp

The (0001) surface of vanadium sesquioxide, V_2O_3, is terminated by vanadyl groups under standard ultra high vacuum preparation conditions. Reduction with electrons results in a chemically highly active surface with a well-defined LEED pattern indicating a high degree of order. In this work we report the first quantitative structure determination of a reduced $V_2O_3(0001)$ surface. We identify two distinct surface phases by STM, one well ordered and one less well ordered. *I*/*V*-LEED shows the ordered phase to be terminated by a single vanadium atom per surface unit cell on a quasi-hexagonal oxygen layer with three atoms per two-dimensional unit cell. Furthermore we compare the method of surface reduction *via* electron bombardment with the deposition of V onto a vanadyl terminated film. The latter procedure was previously proposed to result in a structure with three surface vanadium atoms in the 2D unit cell and we confirm this with simulated STM images.

1 Introduction

The surface structure determines the catalytic activity of heterogeneous catalysts. It is thus indispensable to determine the surface structure of heterogeneous catalysts to develop mechanistic models for catalytic reactions and to systematically improve catalyst materials. Real catalysts are often in powder form and can be studied with techniques such as high resolution transition electron microscopy which can provide detailed information on the catalysts's atomic structure. However, many powerful surface characterization techniques cannot be applied to powder samples. For example, diffraction experiments such as LEED require long range order, while scanning probe microscopy can only be applied to very flat surfaces, precluding industrial powder catalysts from being studied with these methods. Model catalysts reduce the structural complexity and enable application of various characterization techniques. Epitaxially grown thin films of metal oxides on metal or metal oxide single crystals expose extended crystal faces which can be studied in detail. Such surfaces also exist at the faces of micro- or nanoparticles employed in industrial catalysis. Vanadium oxides are widely employed in industrial scale heterogeneous catalysis involving oxygen transfer reactions such as sulfuric acid production and the oxidation of butane to maleic anhydride.[1] V_2O_5 is the thermodynamically stable vanadium oxide under ambient conditions and is usually employed in industrial catalytic applications.[2–5] However under catalytic conditions it is reduced and the active species has a vanadium oxidation state smaller than five.[2] There has been an extended discussion about the surface termination of $V_2O_3(0001)$ films prepared under typical UHV conditions,[6–18] which show catalytic activity in a number of oxidation reactions.[19–24] Recently, we have shown that this surface is terminated by vanadyl groups[25,26] as they are also present on $V_2O_5(001)$ surfaces, however, in tetrahedral and not in pyramidal pentagonal configuration.

The vanadyl oxygen atoms at the $V_2O_3(0001)$ surface can be removed through electron bombardment.[6,13] While the V=O covered surface is unreactive towards a variety of gases, the surface reduced by electron bombardment interacts strongly with a number of molecules and also shows catalytic activity.[19–21] In particular the oxidation of methanol to formaldehyde on this reduced surface has been studied in detail,[22–24] and it was shown that oxygen vacancies in V=O groups are relevant for the reaction. The dominating type of defects under typical UHV preparation conditions are missing vanadyl groups,[27] instead of just missing vanadyl oxygen atoms, and these defects have been shown to not catalyze methanol oxidation.[24]

Despite the number of catalytic studies of the reduced $V_2O_3(0001)$ surface[19–24] there has been no experimental quantitative structure determination of this surface. In this paper we combine *I*/*V*-LEED measurements with STM to determine

Fritz Haber Institute of the Max Planck Society, Faradayweg 4-6, 14195 Berlin, Germany. E-mail: kuhlenbeck@fhi-berlin.mpg.de; Fax: +49 30 8413 3155; Tel: +49 30 8413 4222

† Electronic supplementary information (ESI) available. See DOI: 10.1039/c5cp07390a

the surface structure of the $V_2O_3(0001)$ surface reduced by electron bombardment. This structure is different from the one previously proposed for the $V_2O_3(0001)$ surface reduced by deposition of additional vanadium.[10] We compare the two reduced surfaces obtained by the different approaches and discuss differences and the reasons for these differences. We present STM simulations based on density functional theory (DFT) calculations which confirm the previously proposed structure for the surface reduced by vanadium deposition.

2 Experimental

The experiments have been performed in an Omicron UHV chamber equipped with STM, MCP LEED and other methods. The background pressure of the system was less than 5×10^{-11} mbar and especially before and during reduction experiments a pressure in the 10^{-11} mbar range was maintained to avoid rapid contamination of the reactive reduced surface. V_2O_3 films were grown on an Au(111) single crystal, purchased from MaTeck, Germany, by physical vapor deposition of vanadium in an oxygen atmosphere. The films were ordered *via* multiple annealing steps in oxygen or UHV and the ratio of spot-intensity over background in the LEED patterns was used as a measure to optimize the surface quality prior to the reduction experiments. The Au(111) sample was cleaned by Ar^+ bombardment and annealing. Electron bombardment for surface reduction was carried out with a W-filament placed approximately 1 cm in front of the sample. During reduction the sample temperature was kept below 400 K. For more details of the experimental setup see ref. 26. *I*/*V*-LEED measurements were performed with a stepwidth of 1 eV from 50 eV to 500 eV. Normal incidence of the electron beam to the sample, which is assumed in the *I*/*V*-LEED calculations, was achieved with a Helmholtz coil and confirmed by checking the similarity of *I*/*V*-curves of symmetry equivalent diffraction spots. *I*/*V*-LEED calculations were performed with a modified version of the SATLEED code by A. Barbieri and M. A. van Hove (http://www.icts.hkbu.edu.hk/vanhove). The relativistic phase shifts used in the calculations have been computed for bulk V_2O_3 with the phase shift package supplied with SATLEED. Two different search algorithms were employed to optimize the structure with respect to the Pendry *R*-factor. Initially differential evolution[28] (DE) was used with a maximum angular momentum (LMAX) of 7 and 2 eV step width while the final optimization steps were carried out using CMA-ES with the SHARK library,[29] LMAX = 9 and 1 eV steps. This was done because DE is better at finding the global minimum when the start structure is significantly different to the structure corresponding to the global minimum in R_{Pendry}. CMA-ES on the other hand converges faster when the optimization is started close to the global minimum. Four different types of structural models with one, two or three vanadium atoms or one vanadyl (V═O) group in the surface unit cell were investigated. The number of optimized atomic coordinates and Debye temperatures depends on the model (16 coordinates and four Debye temperatures for the model with one vanadium atom at the surface, 17 coordinates and five Debye temperatures for the models with two vanadium atoms or one vanadyl group at the surface and 18 coordinates and five Debye temperatures for the model with three metal atoms). Additional optimization parameters were in all cases the real and imaginary parts of the inner potential. For each of the metal terminations around 30 different start structures, varying in the interlayer distances, were used as start structures in independent *I*/*V*-LEED optimization runs.

STM simulations were performed with the FHI-aims program package.[30] Electronic structure calculations have been performed with the functional by Perdew and Wang (PW91)[31] using a $10 \times 10 \times 1$ Monkhorst–Pack *k*-grid and tight basis functions as described in ref. 30. We used symmetric slabs generated from the structural data discussed in the Results and discussion section. The surface structure down to the first vanadium layer below the fourth oxygen layer was repeated in reverse order below. This means, the *z*-distances along the surface normal were mirrored while the order, in which the vanadium atoms occupy the sites was kept. In this way slabs of roughly 20 Å thickness were generated. The self-consistent field cycle for the electronic structure calculations was repeated until the total energies of two subsequent runs were different by less than 1×10^{-6} eV. STM images were produced from the electronic structure using the procedure by Tersoff and Hamann.[32] Addition of more basis functions or expanding the *k*-grid to $12 \times 12 \times 1$ did not lead to a noticeable change in the resulting STM pictures. Visualization of the images was done with Visual Molecular Dynamics (VMD).[33]

3 Results and discussion

A number of reduced $V_2O_3(0001)$ surfaces, *i.e.* with a lower oxygen content than the vanadyl terminated surface obtained under standard preparation conditions in UHV, can be envisaged. Two different metal terminated surfaces can be obtained by cutting the bulk V_2O_3 unit cell parallel to the (0001) plane: a surface terminated by one V atom atop a distorted hexagonal O_3 layer, henceforth called single metal (SM) termination, and a surface with two V atoms in the surface unit cell, which we call double metal (DM) termination. DFT calculations by Kresse *et al.* have suggested a surface termination with three V atoms in the surface unit cell, *i.e.* a triple metal (TM) termination.[11] This TM termination was also found experimentally when depositing additional V ontop of a vanadyl terminated surface.[10] These structural models are shown in Fig. 1 together with the vanadyl terminated model structure. Furthermore, in the DFT study mentioned above as well as in another DFT study, reduced surface phases with partial vanadyl coverage were predicted, in which vanadium atoms occupy the sites of missing V═O groups.[11,18]

A vanadyl terminated film was reduced in five steps with *I*/*V*-LEED measurements performed before the reduction procedure and after each reduction step. The *I*/*V*-curves corresponding to the (1 0) diffraction spot are plotted in Fig. 2, with the

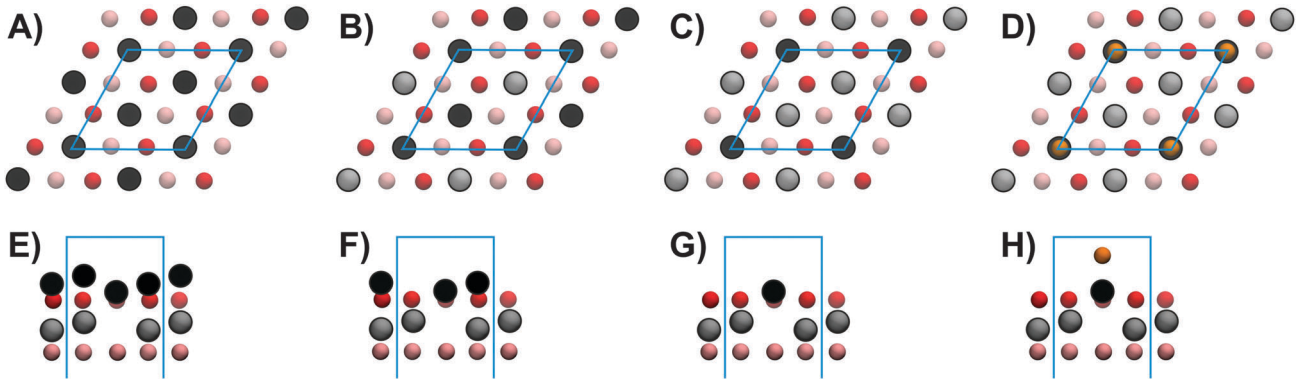

Fig. 1 Structural models of the TM structure (A + E), the DM structure (B + F), the SM structure (C + G) and the V═O terminated structure (D + H). Images (A) through (D) show top views of the respective surfaces while images (E) through (H) show sideviews visualizing the stacking sequence. Color-coding: surface V – black, bulk V – grey, surface O – red, bulk O – pink, vanadyl O – orange; unit cells indicated in blue.

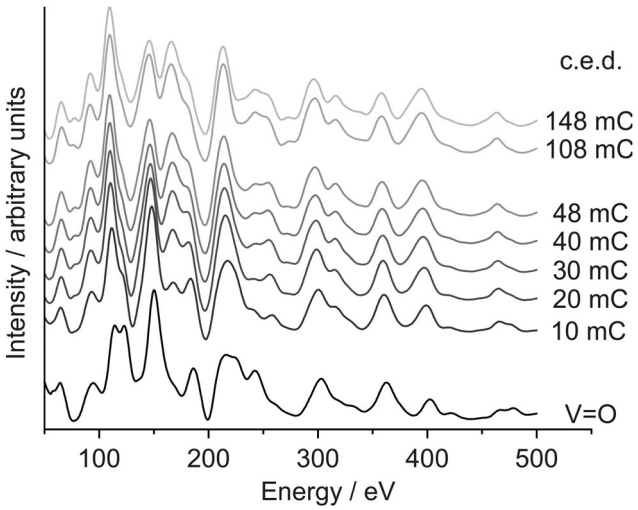

Fig. 2 *I*/*V*-LEED curves showing the stepwise reduction of the V_2O_3(0001) surface. The cumulative electron dose is indicated next to the curves.

cumulative electron dose (c.e.d.) irradiated onto the sample prior to the measurement indicated next to the curves.

I/*V*-LEED calculations for the vanadyl terminated sample (curve labelled V═O) yield a Pendry *R*-factor of 0.09. The sample was then irradiated in five steps with electron doses (E_{kin} = 500 eV) of 10 mC per step (8 mC for the last reduction step). There is a significant change of the *I*/*V*-curve after the first electron dose. For example out of the two peaks at 125 eV that have similar intensities for the V═O terminated surface one shows increased intensity while the other one is reduced to a shoulder after the initial reduction step. Changes in the *I*/*V*-curves are discernible up to a c.e.d. of 40 mC while the curves measured after the last reduction step, corresponding to a c.e.d. of 48 mC, are practically identical to those measured after a c.e.d. of 40 mC. This might be interpreted as a sign of finished reduction, insofar as further electron bombardment does not seem to change the surface structure. Additional reduction experiments on vanadyl terminated V_2O_3(0001) films with doses of 108 mC (E_{kin} = 50 eV) and 145 mC (E_{kin} = 500 eV), both applied in a single dose, also generated *I*/*V*-curves very similar to those obtained after the last two steps of the stepwise reduction (top two curves in Fig. 2).

Table 1 Best-fit Pendry *R*-factors for the fully reduced surface. The two numbers given for the DM termination relate to different settings for the optimization of the Debye temperature of the second surface vanadium atom. Details are given in the text

Surface termination	R_{Pendry}
Triple metal	0.32
Double metal	0.18/0.22
Single metal	0.19
Vanadyl	0.19

I/*V*-LEED calculations gave the best-fit Pendry *R*-factors listed in Table 1 after structural optimization (the dataset obtained after 40 mC cumulative electron dose in the stepwise reduction was used in the *I*/*V*-LEED evaluation). The variation ranges for the Debye temperatures in the *I*/*V*-LEED optimization runs were limited to 550–600 K and to 600–650 K for bulk vanadium and oxygen, respectively. These ranges correspond to the bulk Debye temperatures determined for vanadyl terminated V_2O_3(0001) previously.[26] Without restriction unphysically low bulk Debye temperatures were obtained while the respective Pendry *R*-factors are on average 0.01 smaller than with restriction to physically sensible values. The triple metal termination gives an *R*-factor of 0.32, significantly worse than the results for the other three models, and it is thus unlikely, that this model is the right one. The other three surface terminations yield very similar *R*-factors of 0.19 for the single metal, 0.18 for the double metal and 0.19 for a vanadyl termination model. While the Debye temperature for the vanadium atom ontop of the top oxygen trilayer is around 200 K for all three of those models, the Debye temperature for the second vanadium atom in the DM termination is just 102 K (the lower limit set in the optimization procedure was 100 K). This might be an indication that the DM model does not correspond to the actual surface structure as an artificially low Debye temperature corresponds to strong vibration of this atom, reducing its influence on the *I*/*V*-curves. Furthermore two independent optimizations for DM model

structures resulted in almost identical parameters and *R*-factors (0.184 and 0.187 respectively) but significantly different V–V interlayer distances of 0.68 Å and 0.96 Å between the two surface vanadium atoms. This is also attributed to the limited influence of this atom onto the *I*/*V* data. Limiting the Debye temperature for all atoms to a minimum of 200 K leads to an *R*-factor of 0.22 for the DM model.

The relatively low *R*-factor of the vanadyl terminated structural model could indicate that reduced and V=O terminated areas coexist on the surface. In order to check this, *I*/*V*-LEED calculations with modified experimental data were performed. In these curves certain percentages of V=O coverage were simulated *via* subtraction of *I*/*V*-curves of a vanadyl terminated surface from the experimental data measured for the reduced surface. Partial vanadyl coverages of 10%, 20%, 30%, 40% and 50% were simulated for all three metal terminations. The result was in all cases an increase of *R*-Pendry with increasing V=O admixture, rendering the existence of V=O covered areas unlikely. This is in agreement with the fact that additional electron bombardment does not change the *I*/*V*-LEED curves noticeably which indicates that essentially all vanadyl groups have been reduced. Vibrational spectroscopy of the fully reduced surface also indicates that all vanadyl groups are reduced, as the V=O stretch mode at 127 meV disappears completely.[22]

The STM image of the reduced $V_2O_3(0001)$ surface shown in Fig. 3 reveals the coexistence of two different types of surface termination. The flat areas exhibit round features with a spacing identical to that of the vanadyl terminated surface but with a much lower corrugation of around 0.4 Å. The rougher areas have a corrugation of around 1.2 Å. In some areas the features appear to be somewhat ordered with a structure resembling a $(\sqrt{3} \times \sqrt{3})R30°$ supercell relative to the (1×1) vanadyl termination. The corresponding unit cells are indicated in Fig. 3 with closed (flat area) or broken (rough area) lines. It should be noted that LEED images do not show any visible reflexes of a $(\sqrt{3} \times \sqrt{3})R30°$ supercell indicating that the areas with this structure are too small to produce clearly visible LEED intensity maxima. Consequently in the remaining discussion the focus is on the structure of the flat areas.

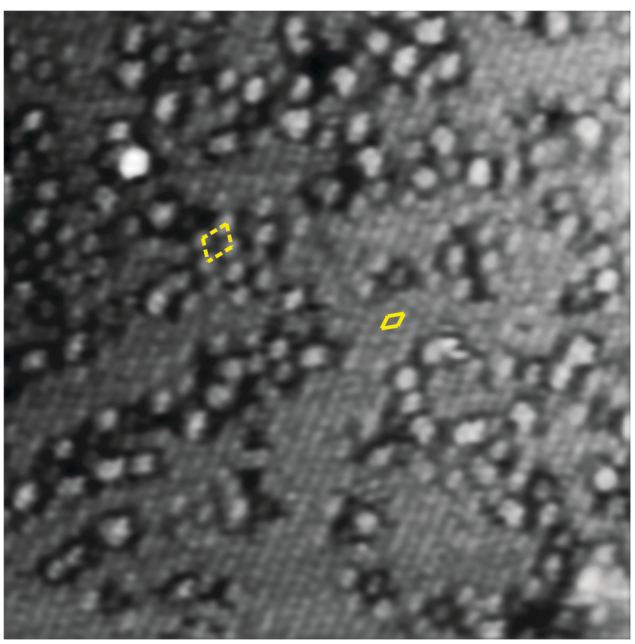

Fig. 3 20 nm × 20 nm STM image of the reduced $V_2O_3(0001)$ surface (145 mC c.e.d.), +1 V, +0.1 nA. The apparent unit meshes are indicated by rhombi drawn with full (flat surface) and broken (rough surface) lines. The image has been FFT-filtered. See the ESI† for the raw image and Fourier transforms.

The triple metal termination can be excluded as the correct structural model for the flat surface areas based on the significantly worse *R*-factor compared to the other three terminations. The double metal termination is rejected based on the very low Debye temperature for the second surface vanadium atom calculated in the *I*/*V*-LEED optimizations and the fact that limiting this Debye temperature to a minimum value of 200 K results in a significantly worse *R*-factor. The vanadyl termination can be counted out based on vibrational spectroscopy, the lack of change in the *I*/*V*-curves after 40 mC cumulative electron dose and the low corrugation in the STM images. We thus conclude that the reduced surface is terminated by a single layer of vanadium atoms atop a distorted hexagonal oxygen trilayer. This termination can be produced from the vanadyl terminated surface simply by removal of the vanadyl oxygen atoms. The rough areas visible in STM might be the result of oxygen atoms removed from the underlying oxygen trilayer by electron bombardment. Previous STM studies of a surface reduced with a smaller electron dose show a smaller amount of disordered surface area indicating that this disordered phase grows with prolonged electron irradiation.[22]

Table 2 lists the interlayer distances in the best-fit SM structure together with the interlayer distances obtained in DFT calculations and the respective changes relative to the corresponding distances in the bulk structure. The distance between the top vanadium atom and the topmost oxygen trilayer is contracted by 45% in the best-fit SM structure. DFT calculations also predict a significant contraction of 64% (GGA) or 55% (HSE). The distance between the topmost O3 layer and the underlying vanadium is changed relatively little in the

Table 2 Interlayer distances in the best-fit SM structure resulting from the *I*/*V*-LEED optimizations in comparison with DFT-results published in references[25] and[11] together with the respective change Δ relative to the bulk interlayer distances

	I/*V*-LEED	Δ (%)	GGA[11]	Δ (%)	HSE[25]	Δ (%)
V_{top}–O	0.54	−45	0.35	−64	0.44	−55
O–V	0.92	−6	1.12	+14	1.00	+2
V–V	0.20	−44	0.22	−39	0.27	−25
V–O	1.15	+17	1.13	+15	1.05	+7
O–V	1.07	+9	1.02	+4	0.91	−7
V–V	0.30	−17	0.38	+6	0.50	+39
V–O	1.07	+9	1.01	+3	0.91	−7
O–V	0.91	−7	0.98	—	0.91	−7
V–V	0.39	+8	(0.36)	—	0.46	+28
V–O	0.95	−3	(0.98)	—	0.91	−7

I/*V*-LEED calculations (5% contraction) while GGA and HSE calculations predict an expansion of 14% and 2% respectively. The V–V distance in the following vanadium double layer is reduced by 44% in good agreement with reductions of 39% and 25% in the DFT studies. The distance to the next oxygen trilayer is increased by 17% with respect to the bulk value (15% and 7% respective increases result from the DFT calculations). For the lower lying layers the interlayer distances resulting from the *I*/*V*-LEED calculations show some deviations from the DFT calculations. Overall the changes of the interlayer distances relative to the bulk values become smaller with increasing distance from the surface and the agreement between experiment and theory is good. The trend for expansion or contraction of the interlayer distances for the five layers closest to the surface is very similar to that for the vanadyl terminated surface,[26] the magnitude of the changes however is larger for the reduced surface. Graphs showing all experimental *I*/*V*-curves for the unreduced surface and the reduced surface after 40 mC c.e.d. as well as the calculated beams for the best-fit structures for a vanadyl terminated model (unreduced surface) and a single metal termination (reduced surface) can be found in the ESI.†

The parameters (V═O model structure) determined for the vanadyl terminated surface match those published previously[26] very well. For the case of the reduced surface we have shown that it is terminated by a vanadium layer with a single atom in the 2D surface unit cell. However, different from the case of the vanadyl terminated surface, in this case three structural models (SM, DM, and V═O) gave very similar *R*-factors so that additional arguments were required to identify the real termination. The reason for this result is likely the limited quality of the fit using the SM model in combination with the higher number of fit parameters for the V═O and the DM models. The VO structure and the DM structure both have one atom more than the SM structure. This corresponds to two additional fit parameters: one interlayer distance and one additional Debye temperature. The optimization algorithm adapts these parameters such that, together with small changes of the other parameters, a good fit results also for the DM and the V═O model, which would not be the case if the fit was better for the correct model. With increasing quality of the fit for the correct structure model the differences between the *R*-factors obtained for this model and for other models get larger as shown previously for very well ordered V═O covered surfaces.[26] For these surfaces the *R*-factor for the vanadyl terminated model is rather small (≈ 0.1) and the difference in *R*-factor between a vanadyl terminated model structure and a single or double metal termination is significant (roughly 0.1 difference in R_{Pendry} for the SM model and 0.2 for the DM model). A solution to the issue of similar *R*-factors for different structural models would be to increase the total energy range of the LEED data since the fit will get worse with increasing energy range for a wrong model. Unfortunately, increasing the energy range was technically not possible in our experiments.

We now turn to the comparison of two different methods of reducing the $V_2O_3(0001)$ surface. In contrast to our method of reduction through electron bombardment the vanadyl terminated surface can also be reduced by depositing additional vanadium as done by Schoiswohl and coworkers.[10] The deposition of additional vanadium leads to coexisting surface structures with one of the two different types of surface-structure having a similarly low corrugation as the flat areas in the STM image of the $V_2O_3(0001)$ surface reduced by electron bombardment shown in this work. However, high resolution STM images of this flat area show that the spacing between the protrusions corresponds to $1/\sqrt{3}$ that of the regular vanadyl terminated surface lattice parameter. It was concluded that the surface prepared by vanadium deposition onto the vanadyl terminated surface contains three metal atoms per surface unit cell. This is also indicated by the attenuation of the (1 0) type spots in LEED and the simultaneous increase in the intensity of diffraction spots corresponding to the $(1/\sqrt{3} \times 1/\sqrt{3})R30^\circ$ unit cell. There is no such systematic attenuation of the (1 0) type spots when reducing the $V_2O_3(0001)$ surface by electron bombardment.

Schoiswohl *et al.* have reported that the surface reduced by deposition of additional vanadium can be ordered by flash-annealing the film to 700 K.[10] More specifically the flat areas, attributed to a metal termination, grow at the expense of the rougher surface areas. For the surface reduced by electron bombardment this procedure leads to a significant decrease of order as seen in LEED images (not shown here). Prolonged annealing in UHV leads to restoring of the vanadyl terminated surface for the surface reduced by vanadium deposition as well as for the surface reduced by electron bombardment. This is in agreement with DFT studies which predict the metal terminated surfaces to be thermodynamically unfavored even at the lowest pressures achievable in UHV systems.[11,25]

STM images have been computed for the four different models using the approach by Tersoff and Hamann[32] applied to electronic structures calculated with DFT as described in the experimental part. The pictures shown in Fig. 4 have been calculated for the structural parameters resulting from the *I*/*V*-LEED calculations corresponding to the *R*-factors in Table 1 for SM, DM and VO models. For the 3M termination model structural data from DFT calculations by Kresse *et al.*[11] were used instead since the *I*/*V*-LEED calculations only give very bad agreement between experiment and theory. Each image shows nine unit cells. First of all it should be noted, that at imaging conditions comparable to our STM measurements (+1 V, 0.1 nA) and previous STM measurements[13,22] (−1 V/+2 V and 0.2 nA), all four structural models give a single round protrusion per unit cell. The simulated STM images thus do not contribute to the identification of the $V_2O_3(0001)$ surface reduced by electron bombardment in this study. The images shown in Fig. 4 have been computed for a voltage of +0.1 V and relatively high isovalues (the isovalue is proportional to the tunneling current). This means that the virtual STM tip is very close to the surface. These simulation conditions match the experimental conditions in STM measurements on the $V_2O_3(0001)$ surface reduced by vanadium deposition.[10] At these conditions the three metal terminations result in distinctly different STM images. The triple metal termination shown in

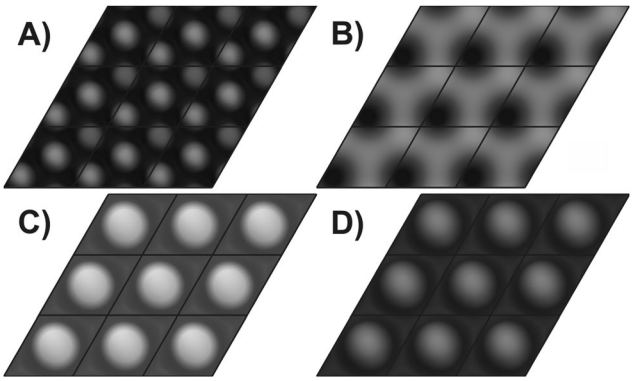

Fig. 4 Simulated STM images for (A) TM, (B) DM, (C) SM and (D) V=O structures; bias +0.1 V; each image shows nine unit cells.

Fig. 4A shows three round protrusions per unit cell. This is in agreement with the experimental images observed by Schoiswohl *et al.* and corroborates their conclusion that the $V_2O_3(0001)$ surface reduced by vanadium deposition is terminated by three vanadium atoms in the surface unit cell. The double metal termination [Fig. 4B] shows two features in the surface unit cell, one slightly more intense than the other, corresponding to the height difference between these two vanadium atoms. The single metal termination [Fig. 4C] shows just a single round protrusion per surface unit cell. In each of the three metal termination simulations the protrusions show up at the positions of the surface vanadium atoms. Finally, the simulation of the vanadyl terminated structure [Fig. 4D][9] also shows one round protrusion per unit cell, as observed experimentally for non-reduced $V_2O_3(0001)$ films.[10,25,26] Previous STM simulations by others also showed one round protrusion per surface unit cell for the V=O termination[18,34] while they did not consider any of the metal terminations.

4 Conclusions

We have shown that reducing the $V_2O_3(0001)$ surface through electron bombardment leads to a coexistence of two surface structures: a badly ordered and an ordered phase. While currently only speculations can be made as to the nature of the badly ordered phase, we have quantitatively determined the structure of the ordered phase. It is terminated by a single vanadium atom in the surface unit cell, similar to the V=O terminated surface with the vanadyl oxygen atoms removed. The interlayer relaxations in the structure with the reduced surface are even larger than in the corresponding vanadyl terminated structure according to *I*/*V*-LEED.

The mediocre R_{Pendry} of 0.18 for this structure is most likely related to the overall limited quality of the surface with significant amounts of disordered areas. The relatively low Pendry *R*-factors of 0.18 for the double metal termination and 0.19 for the vanadyl termination show how the optimization algorithms can fit even an incorrect model to the experimental data with the help of additional free parameters. Increasing the Debye temperature for the topmost vanadium atom in the double metal termination leads to an increase of R_{Pendry} to 0.22.

We have shown that the structure of the reduced $V_2O_3(0001)$ surface depends on the preparation method. The surface reduced by deposition of additional vanadium is terminated by three rather than one metal atoms in the surface unit cell. Our simulated STM images confirm the match of the STM images obtained by Schoiswohl *et al.* with the triple metal structure calculated by Kresse *et al.* by DFT.[10,11]

Both of the different reduced surfaces are only kinetically stabilized and revert to the vanadyl terminated surface upon annealing by oxygen diffusion from the bulk to the surface. This is in agreement with density functional theory predicting the thermodynamic instability of the reduced surfaces even at the lowest pressures achievable in UHV experiments.[11,25]

Acknowledgements

The authors thank Sergey Levchenko for help in setting up the FHI-aims software and for help in performing DFT calculations and STM simulations and Georg Kresse for providing structural data for the triple metal termination. This work was funded by the Deutsche Forschungsgemeinschaft (DFG) within the collaborative research center 546, ''Transition Metal Oxide Aggregates''. We gratefully acknowledge the Fonds der Chemischen Industrie for financial support. Modified versions of the SATLEED code by Barbieri/Van Hove were used in the *I*/*V*-LEED calculations.

References

1 B. M. Weckhuysen and D. E. Keller, *Catal. Today*, 2003, **78**, 25–46.
2 G. L. Simard, J. F. Steger, R. J. Arnott and L. A. Siegel, *Ind. Eng. Chem.*, 1955, **47**, 1424–1430.
3 S. Kasaoka, E. Sasaoka and H. Iwasaki, *Bull. Chem. Soc. Jpn.*, 1989, **62**, 1226–1232.
4 G. C. Bond and S. F. Tahir, *Appl. Catal.*, 1991, **71**, 1–31.
5 G. Deo and I. E. Wachs, *J. Catal.*, 1993, **146**, 323–334.
6 A.-C. Dupuis, M. Abu Haija, B. Richter, H. Kuhlenbeck and H.-J. Freund, *Surf. Sci.*, 2003, **539**, 99–112.
7 I. Czekaj, M. Witko and K. Hermann, *Surf. Sci.*, 2003, **525**, 46–56.
8 I. Czekaj, K. Hermann and M. Witko, *Surf. Sci.*, 2003, **525**, 33–45.
9 H. Niehus, R.-P. Blum and D. Ahlbehrendt, *Surf. Rev. Lett.*, 2003, **10**, 353–359.
10 J. Schoiswohl, M. Sock, S. Surnev, M. Ramsey, F. Netzer, G. Kresse and J. Andersen, *Surf. Sci.*, 2004, **555**, 101–117.
11 G. Kresse, S. Surnev, J. Schoiswohl and F. P. Netzer, *Surf. Sci.*, 2004, **555**, 118–134.
12 T. K. Todorova, M. V. Ganduglia-Pirovano and J. Sauer, *J. Phys. Chem. B*, 2005, **109**, 23523–23531.
13 S. Guimond, M. Abu Haija, S. Kaya, J. Lu, J. Weissenrieder, S. Shaikhutdinov, H. Kuhlenbeck, H.-J. Freund, J. Döbler and J. Sauer, *Top. Catal.*, 2006, **38**, 117–125.

14 E. A. Kröger, D. I. Sayago, F. Allegretti, M. J. Knight, M. Polcik, W. Unterberger, T. J. Lerotholi, K. A. Hogan, C. L. A. Lamont and D. P. Woodruff, *Surf. Sci.*, 2007, **601**, 3350–3360.
15 C. Kolczewski, K. Hermann, S. Guimond, H. Kuhlenbeck and H.-J. Freund, *Surf. Sci.*, 2007, **601**, 5394–5402.
16 J. Seifert, E. Meyer, H. Winter and H. Kuhlenbeck, *Surf. Sci.*, 2012, **606**, L41–L44.
17 A. J. Window, A. Hentz, D. C. Sheppard, G. S. Parkinson, H. Niehus, D. Ahlbehrendt, T. C. Q. Noakes, P. Bailey and D. P. Woodruff, *Phys. Rev. Lett.*, 2011, **107**, 016105.
18 A. Window, A. Hentz, D. Sheppard, G. Parkinson, D. Woodruff, W. Unterberger, T. Noakes, P. Bailey, M. Ganduglia-Pirovano and J. Sauer, *Surf. Sci.*, 2012, **606**, 1716–1727.
19 M. Abu Haija, S. Guimond, Y. Romanyshyn, A. Uhl, H. Kuhlenbeck, T. Todorova, M. V. Ganduglia-Pirovano, J. Döbler, J. Sauer and H.-J. Freund, *Surf. Sci.*, 2006, **600**, 1497–1503.
20 M. Abu Haija, S. Guimond, A. Uhl, H. Kuhlenbeck and H.-J. Freund, *Surf. Sci.*, 2006, **600**, 1040–1047.
21 A. Bandara, M. Abu Haija, F. Höbel, H. Kuhlenbeck, G. Rupprechter and H.-J. Freund, *Top. Catal.*, 2007, **46**, 223–230.
22 Y. Romanyshyn, S. Guimond, H. Kuhlenbeck, S. Kaya, R. P. Blum, H. Niehus, S. Shaikhutdinov, V. Simic-Milosevic, N. Nilius, H.-J. Freund, M. V. Ganduglia-Pirovano, R. Fortrie, J. Döbler and J. Sauer, *Top. Catal.*, 2008, **50**, 106–115.
23 D. Göbke, Y. Romanyshyn, S. Guimond, J. M. Sturm, H. Kuhlenbeck, J. Döbler, U. Reinhardt, M. V. Ganduglia-Pirovano, J. Sauer and H.-J. Freund, *Angew. Chem., Int. Ed.*, 2009, **48**, 3695–3698.
24 Y. Romanyshyn, S. Guimond, D. Göbke, J. M. Sturm, H. Kuhlenbeck, J. Döbler, M. V. Ganduglia-Pirovano, J. Sauer and H.-J. Freund, *Top. Catal.*, 2011, **54**, 669–684.
25 F. E. Feiten, J. Seifert, J. Paier, H. Kuhlenbeck, H. Winter, J. Sauer and H.-J. Freund, *Phys. Rev. Lett.*, 2015, **114**, 216101.
26 F. E. Feiten, H. Kuhlenbeck and H.-J. Freund, *J. Phys. Chem. C*, 2015, **119**, 22961–22969.
27 N. Nilius, V. Brázdová, M.-V. Ganduglia-Pirovano, V. Simic-Milosevic, J. Sauer and H.-F. Freund, *New J. Phys.*, 2009, **11**, 093007.
28 V. B. Nascimento and E. W. Plummer, *Mater. Charact.*, 2015, **100**, 143–151.
29 C. Igel, V. Heidrich-Meisner and T. Glasmachers, *J. Mach. Learn. Res.*, 2008, **9**, 993–996.
30 V. Blum, R. Gehrke, F. Hanke, P. Havu, V. Havu, X. Ren, K. Reuter and M. Scheffler, *Comput. Phys. Commun.*, 2009, **180**, 2175–2196.
31 J. P. Perdew, J. A. Chevary, S. H. Vosko, K. A. Jackson, M. R. Pederson, D. J. Singh and C. Fiolhais, *Phys. Rev. B: Condens. Matter Mater. Phys.*, 1992, **46**, 6671–6687.
32 J. Tersoff and D. R. Hamann, *Phys. Rev. B: Condens. Matter Mater. Phys.*, 1985, **31**, 805–813.
33 W. Humphrey, A. Dalke and K. Schulten, *J. Mol. Graphics*, 1996, **14**, 33–38.
34 S. Surnev, G. Kresse, M. Sock, M. G. Ramsey and F. P. Netzer, *Surf. Sci.*, 2001, **495**, 91–106.